



City Research Online

City, University of London Institutional Repository

Citation: Khan, S. & Finkelstein, L. (2011). Mathematical modelling in measurement and instrumentation. *Measurement and Control*, 44(9), pp. 277-282. doi: 10.1177/002029401104400904

This is the accepted version of the paper.

This version of the publication may differ from the final published version.

Permanent repository link: <https://openaccess.city.ac.uk/id/eprint/14381/>

Link to published version: <https://doi.org/10.1177/002029401104400904>

Copyright: City Research Online aims to make research outputs of City, University of London available to a wider audience. Copyright and Moral Rights remain with the author(s) and/or copyright holders. URLs from City Research Online may be freely distributed and linked to.

Reuse: Copies of full items can be used for personal research or study, educational, or not-for-profit purposes without prior permission or charge. Provided that the authors, title and full bibliographic details are credited, a hyperlink and/or URL is given for the original metadata page and the content is not changed in any way.

City Research Online:

<http://openaccess.city.ac.uk/>

publications@city.ac.uk

Mathematical Modelling in Measurement and Instrumentation

S.H. Khan and L. Finkelstein
Measurement and Instrumentation Centre
School of Engineering
City University, London EC1V 0HB

Abstract

This paper presents a brief outline of the use of mathematical modelling techniques in measurement and instrumentation systems and sub-systems. Following an overview of various models, it illustrates some of the recent advances in mathematical modelling of sensors and instrument transducers. This is illustrated in two case studies describing the use of numerical finite element (FE) modelling techniques for CAD and performance modelling of capacitive sensors and torque motor actuators.

Introduction

Mathematical modelling is a key enabling tool in the analysis and design of measurement systems and measuring instrumentation. It is a method of describing the functioning of instruments and enables principles of instruments to be economically described. Models are a useful basis of instrument element classification. They are a means by which the functioning of systems and equipment can be predicted from a description of its geometry, dimensions and material properties.

This paper will briefly outline the current state of the use of mathematical modelling of measurement and instrumentation systems and will illustrate recent advances in the mathematical models of sensors and actuators by presenting two case studies.

Mathematical modelling in measurement and instrumentation has been reviewed comprehensively by Abdullah¹ and the place of modelling in measurement science, by Finkelstein².

Measuring instrumentation system

It is convenient to discuss the fundamental principles of instruments and of the measurement process in terms of the architecture of a measuring instrument system. Such a system is shown in Figure 1. The system consists of a number of sub-systems. There is firstly the system under measurement. This is connected to a sensor system and acts on the sensor by a flow of matter or energy. The sensor converts this flow into a signal, maintaining a functional relation between the input flow and the information carrying characteristics of the signal. There is usually a signal conditioning bloc which converts this signal into a symbol which may be conveniently handled by the following bloc, which performs any required functions of information transformation and communication. This system passes the information to the effector bloc, to further processing or to the human operator. The effector may be an actuator. The measuring instrument system operates under the control of a control bloc. An important part of the system is the human-machine interface. Through this interface the operator effects supervisory control of the measurement process. The interface embodies also any displays.

In the great majority of modern systems once information has been acquired by a sensor and conditioned, it is processed and effectuated by standard computing equipment. The control of the measurement process and the display of information to the operator also take place through standard human computer interfaces. Thus much of instrumentation is implemented by modern computer equipment.

Special problems of modelling of measurement systems

That part of modern instrumentation systems, which is implemented using standard information technology, is modelled using the techniques of signals and information systems science. The equipment is generally built up of standard functional blocs and is modelled using functional models such as transfer functions and the like¹.

This paper will not consider this aspect of instrumentation system modelling, but will consider the aspect of modelling unique to measurement instrumentation. The modelling of sensors and actuators and of the interaction between the sensor and the measured system must be carried out considering the embodiment of those systems, that is their geometry, dimensions and material properties. It is this modelling which presents challenging problems. Unlike much such system modelling in control, the models require to be very accurate. Modern methods of modelling enable this accuracy to be achieved.

Idealised embodiment models

The relation between an element physical embodiment and its function can be represented by idealised lumped parameter models. Finkelstein and Watts³ presented the principles of such representation. It is widely used in systematic approaches to measurement science².

Such models have their origin in electrical circuit analysis. They are based on the relation between the input power flow to an element, or system, and the output flow. Power flow is modelled by pairs of conjugate variables, the product of which is power: voltage and current, force and linear velocity, torque and angular velocity, pressure and flow, temperature and heat flow rate (or more correctly entropy flow rate), and the like. The power is input and output to objects at points termed ports. Physical objects perform one of the following elementary operations on the input power: (i) storage, (ii) transformation, including conversion from one form of energy into another, (iii) transmission without change and (iv) modulation or control, in which a physical signal variable modulates or controls the power processes in the object without itself exchanging power with them.

The idealised models take the form of relations between the power flow variables of the object acting as variables of the model, with the physical quantities characterizing the energy processes acting as parameters. The relations take usually the form of differential equations. For linear, or linearised relations representation in the frequency domain, using transfer functions, is particularly convenient.

Power flow models of elements using this form of description show far-reaching isomorphisms between models of elements of different physical form. Such models are important for the analysis of instrument elements particularly sensors. They are a convenient form of representation for archetype models, generalized models of a particular class of sensor, representing clearly the principle of operation of elements and providing a means of their classification for incorporation in knowledge bases. They are also significant step in the

derivation of signal flow models from physical models and the estimation of the effect on the measured system of power abstraction by the instrumentation connected to it.

When such models are formulated in transfer function form, there is a variety of computer analytical tools for their analysis, and for the design of systems described by them. MATLAB is a powerful and popular system. There are also highly effective computer tools for the generation and analysis of power flow models of the kind described above. The bond graph technique is outstanding examples.

An example of an idealised model of a simple transducer principle is shown in Figure 2. The transducer schematic embodiment is shown in Figure 2a. The transducer consists of a coil of n turns and of area A . The coil rotates in a magnetic field B . L is the inductance of the coil and R its resistance. J is the moment of inertia of the coil about its axis, and b the damping coefficient. The coil has a mechanical power port, with a torque T and an angular velocity $d\phi/dt$. At the electrical port there is a voltage v and a current i . The coil may act as a transducer of mechanical to electrical signal producing an output signal proportional to angular velocity. Alternatively it may be a transducer of electrical to mechanical signal converting a current to a proportional torque. Figure 2b illustrates an idealized model of the transducer in transfer function, bloc diagram form. It illustrates its principle of operation and general relation of its function to its construction.

Realistic mathematical models

While idealised models are useful in the representation and analysis of concepts and in conceptual design, detailed analysis and design requires models which relate the detailed geometry, dimensions and material properties of the object modelled to its functional behaviour. Engineering objects are characterized by complex geometries and distributed properties. The physical laws governing their behaviour are represented by partial differential equations, which are often non-linear and transcendental.

Analytical solutions of such realistic models are generally not feasible. However finite element techniques have made possible the formulation and analysis of such models. It is in this area that significant progress is being made. The review¹ shows that useful realistic models of this type have been formulated for a variety of types of instrument element: electro-mechanical, elastic deformation and thermal. The models have been employed for practical design. The following sections below illustrate such models by two recent applications.

Modelling of capacitive sensors

Capacitive sensors are extensively used in many applications for measuring displacement, pressure, torque, flow, and other physical quantities^{4, 5, 6}. In all these cases the primary sensor is based on the well-known capacitive technique in which the capacitance in a system of electrodes is changed owing to the redistribution of electric field caused by changes in dielectric properties and/or geometric parameters of the sensor. In general, the performance of a capacitive sensor is dependent upon the electric field distribution between its electrodes which, in turn, depends upon its design parameters and operational regimes (e.g. flow measurement). Consequently, accurate modelling and computation of field distribution is vitally important in order to be able to design sensors that would deliver the required output

characteristics. Here a generic approach to modelling and CAD of capacitive sensors is presented by considering capacitive sensors for flow imaging and angular position sensing.

As shown in Figure 3 the heuristic procedure for FE modelling and design of capacitive sensors comprises three main processes. These are the process of defining and setting up appropriate FE models (pre-processor), the process of solving the defining differential equation (solution-processor), and the process of calculating the necessary output parameters from the solution of the defining equation (post-processor). This procedure is repeated until a satisfactory design is obtained.

For capacitive sensors the defining differential equation is given by the following Laplace's equation⁷ which governs the electric field distribution in the problem domain Ω of the sensor:

$$\nabla \cdot \epsilon \nabla \Phi = 0 \quad \text{in } \Omega \quad (1)$$

Under appropriate boundary conditions the above equation is solved by finite element method (FEM)⁸ in terms of electric potential Φ for given permittivity distribution ϵ . For this, in most cases it is possible to limit the problem domain to 2D region $\Omega(x, y)$ by neglecting any leakage flux or fringing field effects due to the finite length of electrodes. This is especially true for cylindrical arrangements of sensor electrodes with small length to diameter ratio and in sensors where special measures are taken to reduce leakage field effects. In most cases it is also assumed that dielectric materials are linear, piece-wise homogeneous and isotropic. In the presence of charge densities ρ the right hand side of equation (1) is non-zero and the corresponding Poisson's equation $\nabla \cdot \epsilon \nabla \Phi = -\rho$ is solved. Following the solution of equation (1), field intensity and flux density vectors \mathbf{E} and \mathbf{D} , and other quantities like capacitance are calculated. The FE modelling results are normally validated against experimental data. However the accuracy of results may also be verified and evaluated qualitatively and quantitatively by using special numerical techniques⁹.

Since the performance modelling and CAD of capacitive sensors by FE field modelling comprises many simulation 'runs' involving model definition and discretisation, mesh refinement, parameter calculation and error estimation, validation and performance prediction, a systematic modelling approach based on effective modelling methodologies must be adopted. This is to reduce the considerable amount of time and effort needed for simulation studies and to ensure increased accuracy, reliability and comparability of simulation results. For capacitive sensors this may involve the exploitation of any symmetry conditions, reduction of problem domain, adoption of systematic model development and refinement strategies for pre-processing, full automation of analysis 'runs' and post-processing of results, etc.

Realisation of finite element models of capacitive sensors

The modelling strategies discussed above were used to investigate and design two capacitive sensors shown in Figure 4. Figure 4(a) shows the cross-section of a 12-electrode electrical capacitive tomography (ECT) sensor for two-phase flow imaging in real time. It consists of 12 capacitive electrodes mounted symmetrically on the surface of the special insulating section of a pipeline. The earthed radial screens reduce large capacitances between adjacent electrodes and the outer screen (also earthed) - shields stray fields. The spatial distribution of flow components inside the flow pipe is determined by measuring the capacitances between

all possible combination of electrodes and solving the appropriate inverse problem. This is done by applying a constant potential to one of the electrodes and measuring the capacitances between this and the rest of the electrodes. The process is repeated for all electrodes and the capacitance data, thus obtained together with field computation results are used to solve the inverse problem and image the flow component distribution. Beck *at al*¹⁰ first proposed to use the capacitive technique for flow imaging and today ECT has shown considerable potential to be used in industrial tomography for measurement and imaging of various processes in process industry, especially the oil industry. The performance of such an ECT sensor is strongly dependent upon its main design parameters $\delta_1, \delta_2, \delta_3, \delta_4, \theta, \epsilon_1, \epsilon_2$ and number of electrodes N shown in Figure 4(a). Using the modelling strategies mentioned in the previous Section extensive simulation studies were undertaken to design and optimise the above ECT sensor against these design parameters. The resulting industrial prototype was successfully tested and shown to give improved spatial resolution (2%) and better image quality¹¹.

The capacitive sensor shown in Figure 4(b) is used for angular position sensing in limited angle torque motors for frame scanning in infrared thermal imaging devices. It consists of a compact arrangement of four outer electrodes, one cylindrical centre electrode and two rotating electrodes. Potentials of the same magnitude but opposite polarities are given to the outer electrodes while the rotating electrodes are kept at zero potential. The rotating electrodes attached to the motor shaft rotate to change the effective overlap (and hence the field distribution) between the centre and outer electrodes. This changes the capacitance between the electrodes and also the sensor output voltage V measured between the 'floating' centre electrode and the virtual earth. Here the main design variables are the geometric parameters of the electrodes and the dielectric material ϵ_7 , and the output of interest is the magnitude and linearity of the voltage to angular position ($V-\theta$) characteristic. The same modelling methodologies were used to carry out both 2D and 3D simulation studies to investigate the effects of various design parameters and leakage flux on the performance of this large diameter to length ratio sensor. The modelling results were validated against experimental data obtained from industry.

Typical FE models for capacitive sensors described above are shown in Figures 5 and 6. In most cases it is usually sufficient to use 2D models for CAD and simulation studies. There are, however cases in which 3D models are required in order to take into account fully the complex nature of electric field distribution, especially in devices with complicated geometric configuration¹². In addition, sometimes 3D models are also required to justify, both qualitatively and quantitatively, the use of 2D modes for simulation. Such a 3D FE model for the small length-to-diameter ratio angular position sensor is shown Figure 4(b). It contains about 75000 eight-noded hexahedral elements made up of approximately the same number of nodes. For a relatively small size sensor (about 25 mm in length and 17 mm in diameter) this provides modelling accuracy comparable to that of accurate 2D models. Such 3D models were used to investigate the effects of leakage flux in the sensor¹². For boundary conditions either Dirichlet ($\Phi=\Phi_i$) or Neuman ($\partial\Phi/\partial n=k$) boundary condition is used. No boundary condition is imposed on any 'floating' potential regions. However special measures need to be taken to tackle these regions in FE modelling. For example, a novel technique was used for the first time to simulate the 'floating' potential centre electrode in the angular position sensor shown in Figure 4(b)¹³. Since it is a conductor there must not be any electric field inside it ($E=0$) and its surface must comprise an equipotential surface. This condition is satisfied by assigning an infinitely large permittivity value to all FE regions occupied by the centre electrode. Following the FE solution of the field equation (1) the capacitance C between

given electrodes is calculated either from field energy E ($E=CV^2/2$) for a given potential difference V or from charge Q using $C=Q/V$. Here the charge Q is calculated by integrating the flux density vector \mathbf{D} over the appropriate electrode surfaces⁹ using the Gauss's law:

$$Q = \int_S \mathbf{D}_n \cdot d\mathbf{s} = \int_S D \cos \theta \, ds = \int_S \mathbf{D} \cdot \mathbf{n} \, ds = \int_S \mathbf{D} \cdot d\mathbf{s} \quad (2)$$

Obviously any errors in the capacitance calculation are dependent upon the errors associated with the field computation and the numerical integration technique used to calculate the charge Q from equation (2). The FE models shown in Figures 5 and 6 were obtained by using the commercial FE packages OPERA-2d and OPERA-3d used for all modelling purposes¹⁴.

Some modelling results for capacitive sensors

Some of the typical results of simulation in terms of equipotential contour plots and output performance characteristics are shown in Figures 7 and 8. Figure 7(a) clearly shows the shielding effects of the radial screens in reducing the large capacitance values between the adjacent electrodes in the 12-electrode ECT sensor. Many simulation runs involving the radial screen thickness δ_4 , its penetration depth inside the flow pipe δ_3 and the angular size of the electrodes θ are needed to establish the optimum values of these parameters. The nonlinear effect of the flow regime on the spatial distribution of field inside the flow pipe is evident from Figure 7(b). Here, for the two-phase flow of oil (the central shaded region, $\epsilon=3$) and gas (the surrounding air region, $\epsilon=1$), the flow concentration β is defined as the ratio of the cross-sectional area of the higher permittivity component and that of the flow pipe. Figure 8 shows the typical field distribution between the outer and centre electrodes for the angular position sensor shown in Figure 4(b). The magnitude and linearity of its voltage-position characteristic ($V-\theta$) are dependent upon the uniformity of the field distribution and the position and size of the rotating electrodes⁹. Simulation results have shown that the $V-\theta$ characteristic is also critically dependent upon the dielectric property of the inner insulator ring (ϵ_7) between the centre electrode and its carrier (Figure 4(b)). Thus the stability of ϵ_7 which is sensitive to temperature variation is vitally important for the reliable performance of the sensor.

Modelling of torque motor actuators

Limited angle torque motor actuators are specialised electrical motors which find wide application in many servo mechanisms. The actuator presented here is a limited angle torque motor which, unlike conventional electrical motors, only execute 'oscillatory' limited angular deflections with a given frequency. They are used as frame scanners in a wide range of infrared thermal imaging and laser systems. These motors are also ideally suited for aerospace servo-valve control and other similar applications. Figure 9 shows the cross-section of such a torque motor actuator. It consists of a solid iron armature surrounded by the solid stator made of the same ferromagnetic material. The armature is pressed on to the motor shaft made of nonmagnetic stainless steel. The stator consists of two segmented yokes (called the magnet yoke pair) which are fixed in position to the nonmagnetic end plates of the motor containing the bearing housings. The stator windings or excitation coils are wound around the yokes and are connected either in series or in parallel. The external diameter of the armature blades maintains a very small airgap of 0.05-0.07 mm between the armature and stator poles. When the stator windings are unexcited ($I=0$) the magnetic flux produced by two permanent magnets resting on the stator segments produces a 'detent torque' which retains the armature

at $\theta=0$ position shown in Figure 9. Thus the motor has an inherent magnetic stiffness which, in many applications provides for fail safe operation.

For the normal operation of the motor the stator windings are fed by a 50-Hz sawtooth waveform which the motor is required to follow in order to deliver the required 50-Hz scanning frequency (image frame rate) of the mirror attached to one of the shaft ends with a maximum angular frequency of $\pm 8^\circ$. The performance of the motor is very much dependent upon the geometric and chosen material parameters for the stator yokes and armature, and the permanent magnets. The linearity and efficiency of the motor performance during an active scan period is affected by the degree of saturation of its magnetic circuit which, in turn depends on the materials used. Hence the importance of computer-based modelling and investigation, especially when at present there is a requirement for improved linearity of 0.1% during the active scan period and an increased scanning efficiency (active scan/total scan time) of 90%. This is done by modelling and computation of 2D nonlinear magnetic field distributions in the motor for various combinations of geometric and material using FEM.

For all electromagnetic actuators, including the above torque motor actuator, the core modelling activity comprises the solution of the following generic nonlinear Poisson's equation⁸:

$$\text{curl}\left(\frac{1}{\mu} \text{curl}\mathbf{A}\right) + \text{curl}\left(\frac{\mathbf{M}}{\mu_1}\right) = \mathbf{J} - \sigma \frac{\partial \mathbf{A}}{\partial t} + \sigma \mathbf{V} \times (\text{curl}\mathbf{A}) \quad (3)$$

where vectors \mathbf{A} , \mathbf{M} , \mathbf{J} and \mathbf{V} are magnetic vector potential, magnetisation, source current density and velocity respectively. The material parameters μ , μ_1 and σ are magnetic permeability, apparent permeability and conductivity respectively. For a given armature position θ the above equation is solved by FEM. Usually various modelling experiments are carried out to establish the appropriate number, size and distribution of elements that would ensure quick and efficient calculation of such important global parameters as torque, force, and other parameters of practical interest. Following the field computation, the torque/force is calculated by using one of the three methods based on Maxwell stress tensor or virtual work or the magnetising current. In order to increase the overall modelling accuracy about 27000 first-order triangular FE elements were used for the above torque motor actuator. These FE models were used for performance modelling, design optimisation and prediction of such torque motor actuators.

Conclusions

Models, especially mathematical models are a key enabling tool in the analysis and design of measurement systems and measuring instrumentation. With the availability of powerful desktop computers significant progress is now being made in the application of numerical techniques such as finite element method for modelling, CAD, performance prediction and validation of instrument transducers and sensors.

References

1. Abdullah F., Finkelstein L., Khan S.H. and Hill W.J., Modelling in measurement and instrumentation - An overview. *Measurement*, 14, 1994, 41-54

2. Finkelstein L., Measurement and instrumentation science- An analytical review, *Measurement* 14, 1994, 3-14.
3. Finkelstein L. and Watts R. D., 1983, 'Fundamentals of transducers-description by mathematical models, In: P. H. Sydenham (Ed.), *Handbook of Measurement Science*, Chichester: Wiley, vol. 2, pp. 747-795.
4. A. Falkner, A capacitor-based device for the measurement of shaft torque, *IEEE Trans. Instrum. Meas.* **45** (4) (1996) 835-838.
5. X. Li and G. C. M. Meijer, A new method for the measurement of low speed using multiple-electrode capacitive sensor, *IEEE Trans. Instrum. Meas.* **46** (2) (1997) 636-639.
6. F. N. Toth, G. C. M. Meijer, and M. van der Lee, A planar capacitive precision gauge for liquid-level and leakage detection, *IEEE Trans. Instrum. Meas.* **46** (2) (1997) 644-646.
7. J. D. Kraus, *Electromagnetics*, 4th ed., McGraw-Hill Inc., London, 1992.
8. K. J. Binns, P. J. Lawrenson, and C. Trowbridge, *The Analytical and Numerical Solution of Electric and Magnetic Fields*, John Wiley & Sons, Chichester, 1992.
9. S. H. Khan and F. Abdullah, Finite element modelling of multielectrode capacitive systems for flow imaging, *IEE Proceedings-G*, **140** (3) (1993) 216-222.
10. M. S. Beck, A. Plaskowski, and R. G. Green, Imaging for measurement of two-phase flows, in: *Proceedings of the 4th International Symposium on Flow Visualization*, 1986, p. 585-588.
11. M. S. Beck, B. S. Hoyle, and C. P. Lenn, Process tomography in pipelines, *SERC Bulletin*, **4** (10) (1992) 24-25.
12. S. H. Khan, K. T. V. Grattan, and L. Finkelstein, Investigation of leakage flux in a capacitive angular displacement sensor used in torque motors by 3D finite element field modelling, *Sensors and Actuators: A. Physical*, **76** (1999) 253-259.
13. S. H. Khan, L. Finkelstein, and F. Abdullah, Investigation of the effects of design parameters on output characteristics of capacitive angular displacement sensors by finite element field modelling, *IEEE Trans. on Magnetics*, **33** (2) (1997) 2081-2084.
14. OPERA-2d, version 7.035 1998, OPERA-3d version 2.609 and TOSCA version 6.6, 1997, Vector Fields Limited, UK.

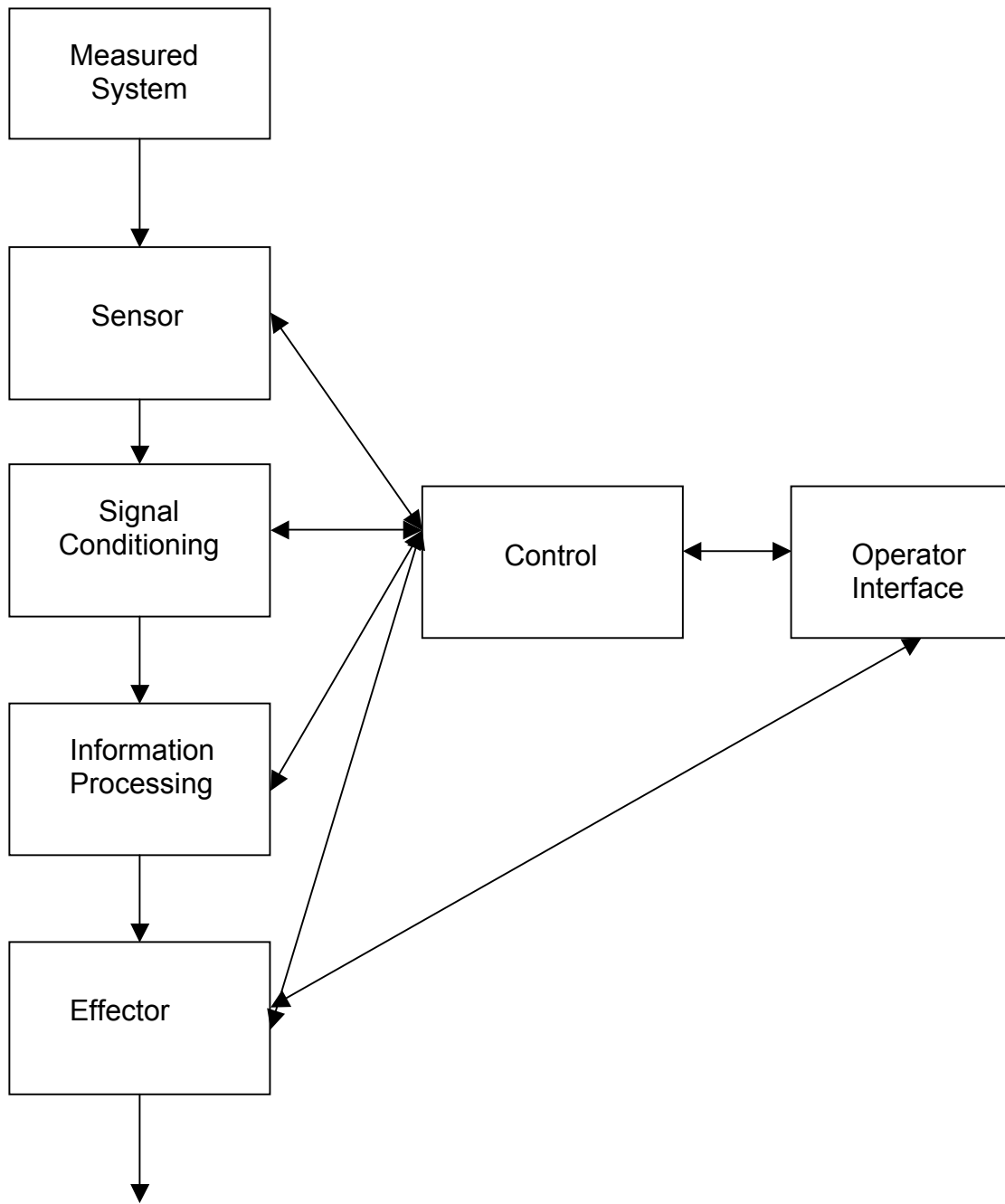


Figure 1: Measuring Instrumentation System

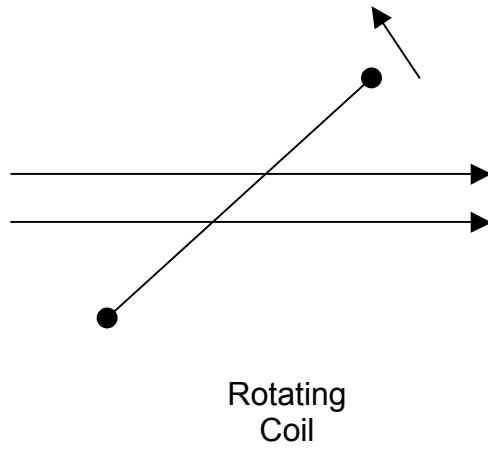


Figure 2a: Coil rotating in a magnetic field

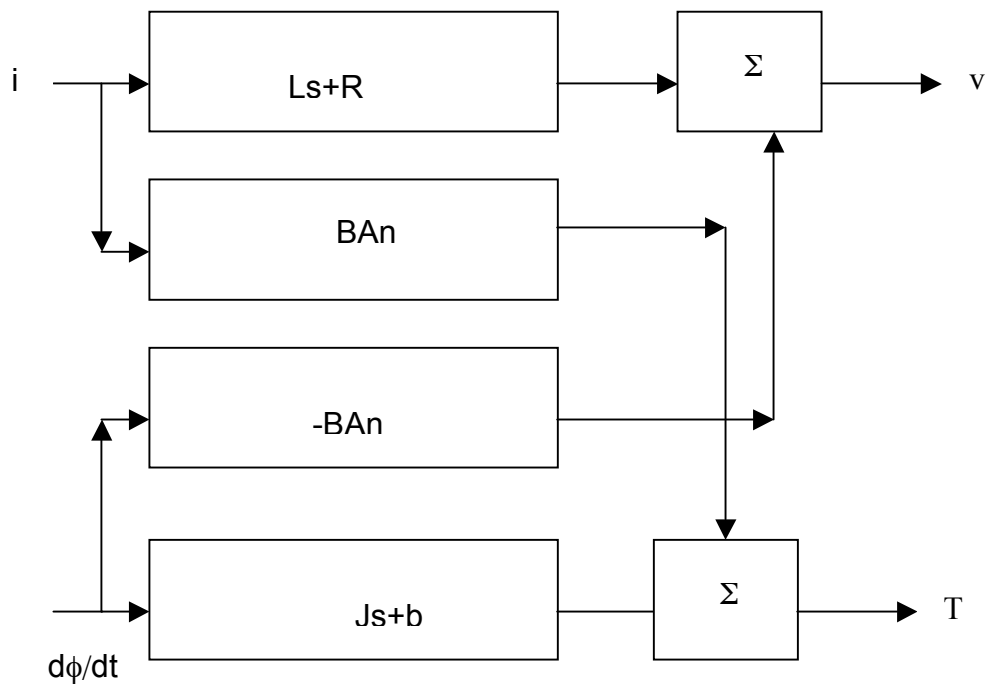


Figure 2b: Mathematical model of transducer

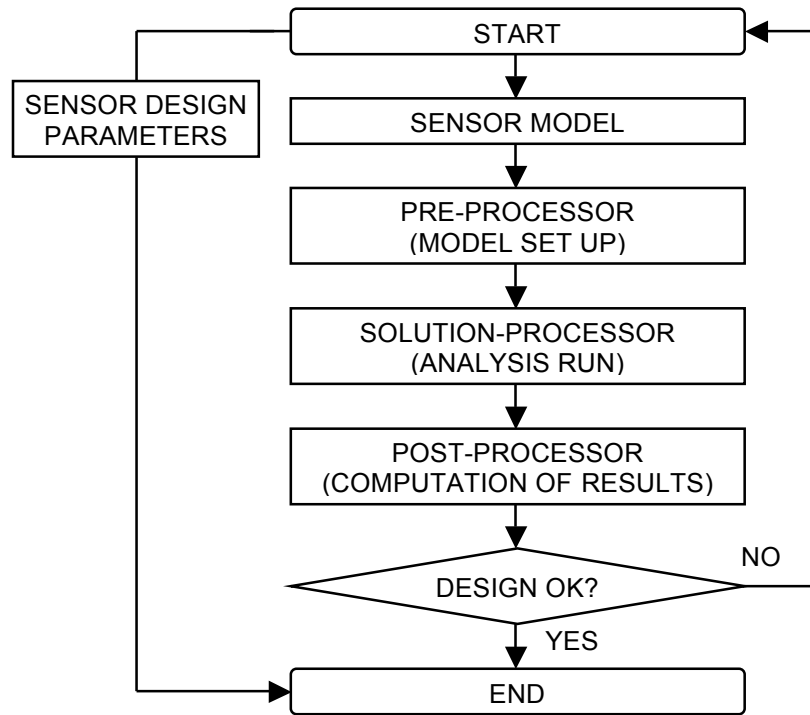


Figure 3: Heuristic sensor design procedure for capacitive sensors

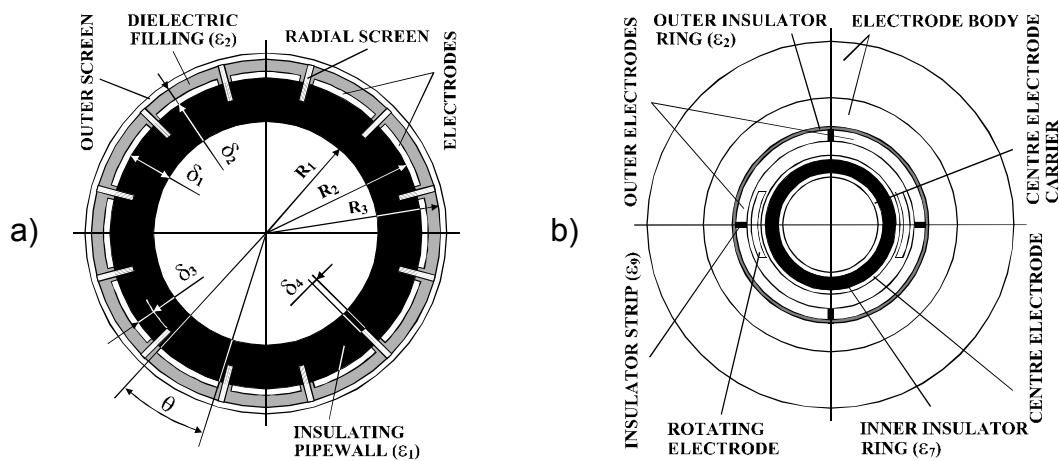


Figure 4: Cross sections of capacitive sensors investigated: (a) 12-electrode electrical capacitive tomography (ECT) sensor for two-phase flow imaging, (b) 4-electrode angular position sensor

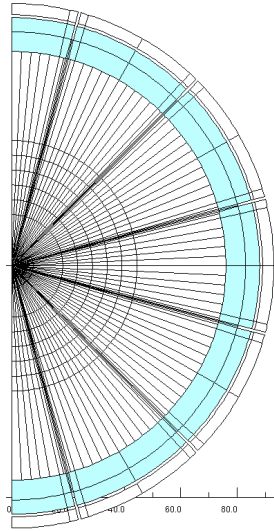


Figure 5: Typical finite element model of the 12-electrode ECT sensor for flow imaging shown in Figure 4(a) (half model).

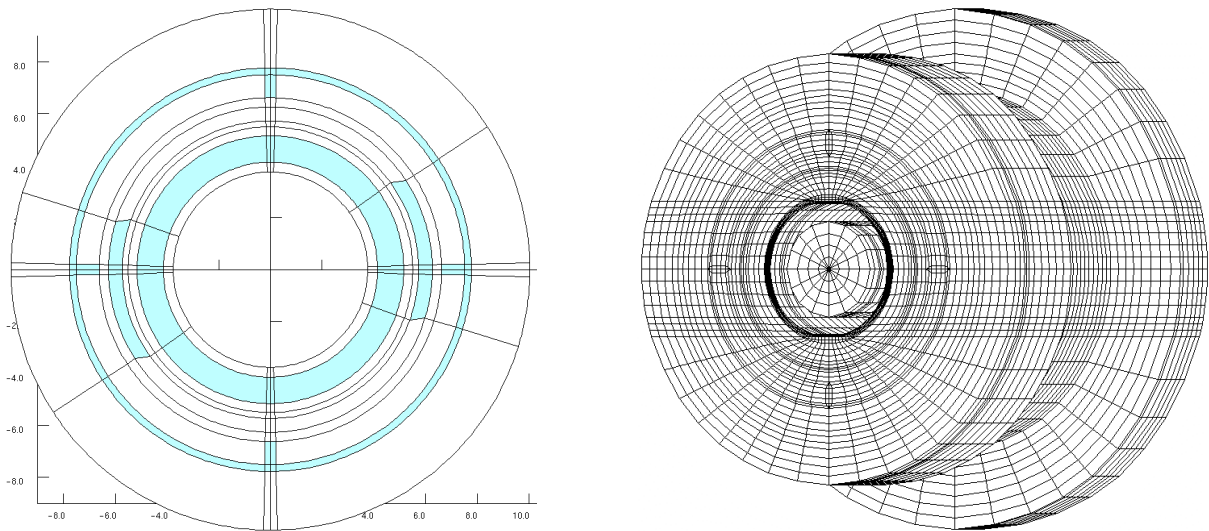


Figure 6: Typical 2D (left) and 3D (right) finite element model of the 4-electrode capacitive angular position sensor shown in Figure 4(b) (full models).

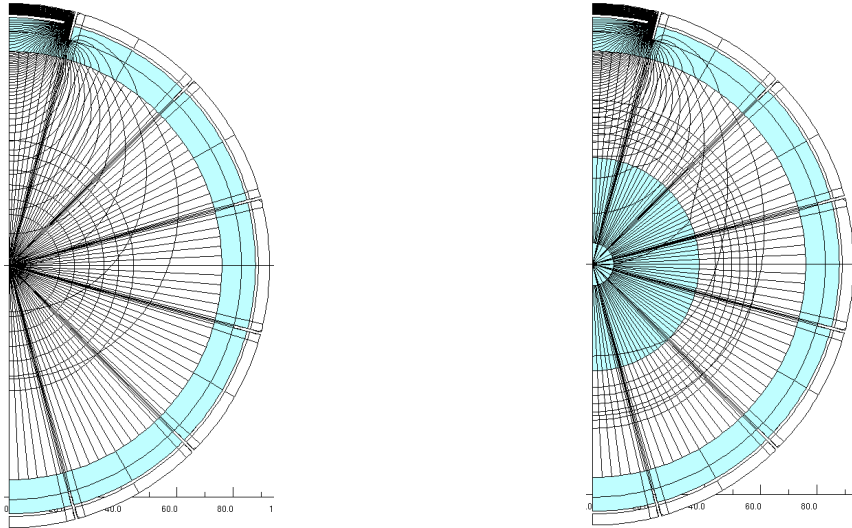


Fig. 7: Equipotential contours in the 12-electrode ECT sensor showing the effects of radial screens (left) and core flow ($\beta=25\%$)(right) on field distribution between the sensor electrodes.

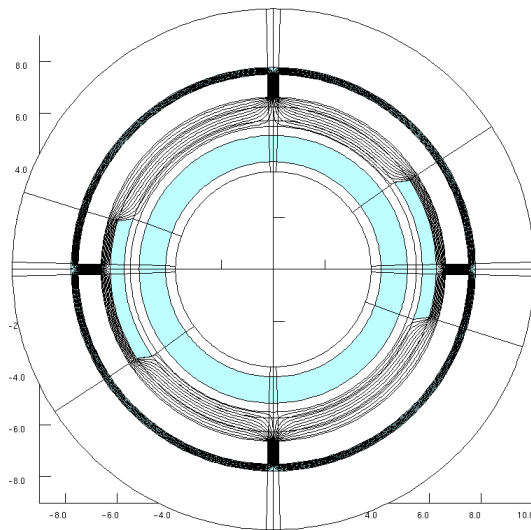


Fig. 8: Equipotential contours in the 4-electrode angular position sensor showing field distribution between the outer and centre electrodes for position $\theta=8^\circ$.

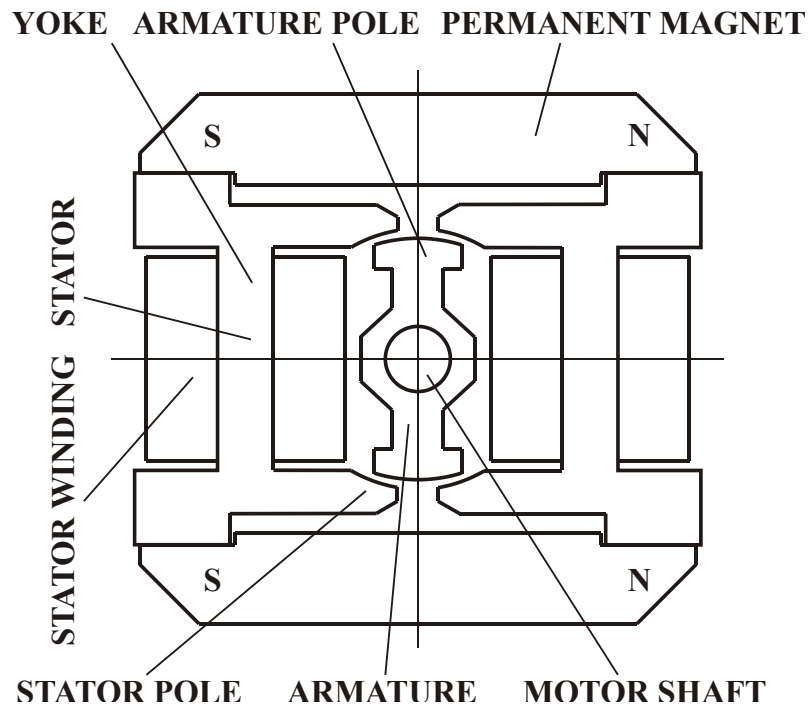


Fig. 9: Cross-section of a two-pole limited angle torque motor actuator used for frame scanning in infrared thermal imaging devices.